Advances in Military Technology
Vol. 20, No. 2, 2025, pp. 449-465
ISSN 1802-2308, eISSN 2533-4123
DOI 10.3849/aimt.01957

Model for Assessing Potential Capabilities of Surface-to-Air Missile Forces Group to Repel Air Attacks

V. Gorodnov*

National Academy of the National Guard of Ukraine, Kharkiv, Ukraine

The manuscript was received on 13 January 2025 and was accepted after revision for publication as an original research paper on 16 October 2025.

Abstract:

To construct the model, a theorem on specific properties of Markov graphs is proven. Based on this, an analytical representation of the model described in the title is derived within the framework of continuous-time, discrete-state Markov processes. The model accounts for the structure of surface-to-air missile systems (SAMS) in ground-based group battle formations, as well as the formations of means of air attack (MAA) in the air. Its validity is confirmed by showing that the analytical model can be reduced to known and previously verified models. The results demonstrate that relying on traditional models can overestimate the effectiveness of SAMS groupings by up to three times, potentially leading to incorrect conclusions about their capability to accomplish combat missions.

Keywords:

battle model, Markov processes, theorem, surface-to-air missile systems

1 Introduction

Anti-aircraft missile forces groups are the most effective means of protecting key government objects, as well as their own ground forces, forces and means from attacks by enemy MAA.

Such groups are armed with surface-to-air missile and missile-artillery (hereinafter referred to as surface-to-air missile) systems (SAMS) with necessary ammunition and means for obtaining intelligence information and target designation information.

The spatial capabilities of each SAMS are limited by the area of air targets effective destruction – the fire zone – and may have areas of overlap with fire zones of neighboring SAMS (Fig. 1).

For ease of presentation, we will introduce a system of notations for necessary variable quantities, which we will use in our further discussions.

The total fire zone of n SAMS grouping in space may have different areas with different SAMS compositions, which can fire at MAA in these areas. In Fig. 1, $n = 4$

*Corresponding author: National Academy of the National Guard of Ukraine, 3 Zakhysnykiv Ukrainy Square, UA-610 01, Kharkiv, Ukraine. Phone: +380 67 954 92 16, E-mail: vgor46@ukr.net

and we denote the probabilities of MAA hitting in each of this sections of general fire zone with symbols R_1, R_2, R_3, R_4, R_{12}, R_{23}, R_{34}, R_{14}, R_{123}, R_{234}, R_{134}, R_{124}, R_{1234}.

Nomenclature	
Probability of occurrence, in the input flow to a SAMS, of an MAA group consisting of exactly r MAAs	b_r
Number of combinations from n to m	C_n^m
Probability of transition to the k-th level of the model graph of SAMS by jumping through q tiers of the graph	d_k^q
Input density function of the MAA flow	$f_1()$
Service duration distribution density function	$f_2()$
Probability deformation function, that modifies the Erlang probability P_k	F_k
Intensity of the MAAs input flow in SAMS grouping	I
Identifiers (numbers) of specific SAMS	$i_1 \ldots i_n$
Maximum total MAAs number in one group	L
Probability of the MAA falls within the service area of j SAMS	l_j
Mathematical expectation of SAMS number engaged in firing at targets	$M_{b.SAM}$
Mathematical expectation of the number of MAAs in one group at the SAMS grouping input	$M_{in.gr}$
Total number of SAMSs in SAMS grouping	n
Total number of objects to be hit during an MAA strike	N_{obj}
Number of typical objects to be hit by a group of r MAA	n_r
Mathematical expectation of the number of aircraft that penetrated the air defense system unopposed	N_{missed}
Total number of enemy aircraft in a single attack	$N_{total.En}$
Probability that exactly k SAMSs are occupied (model state probability)	P_k
Probability that SAMSs with numbers i, j, k are engaged in servicing	$p_{i\,j\,k}$
Probability of MAA servicing within the SAMS grouping (performance indicator)	$P_{service}$
Probability that a Markov process is in the state set X	P_X
Probability that a Markov process is in the state subset Y	P_Y
Probability that a Markov process is in the state subset Z	P_Z
Probability that an MAA falls within the service area of SAMSs with $i_1 \ldots i_m$ numbers	$R_{i_1 \ldots i_m}$
Number of MAAs in one group	r
Number of SAM systems not engaged in firing at enemy aircraft	s
System state where SAMSs with numbers $i_1 \ldots i_k$ are busy in firing at targets	$S_{i_1 \ldots i_k}$
Mathematical expectation of MAA's duration firing time in SAMS	T
Set of graph vertices	X
Subset of graph vertices	Y
Subset of graph vertices	Z
Total area of j-fold overlap of SAMS accessibility zones	z_j
Total service area of MAAs flow in SAMS grouping	z_Σ
Input MAAs flow parameter in SAMS grouping	λ
Partial flow parameter for MAA groups consisting of exactly r MAAs in each group	λ_r
Channel performance in SAMS grouping	μ
Load factor of a SAMS grouping	ρ
Load factor of a SAMS flow of MAA groups consisting of exactly q MAA in a group	ρ_q
Intensity of transition to a group of states with k occupied SAMSs, via a jump over q states	γ_k^q
Intensity of transition from state S_{ij} (SAMSs i, j engaged) to state S_i at level v of the graph	$\gamma_{ij \to ijk}^{v}$
Probability that an MAA falls into the total accessibility zone of exactly j SAMSs	π_j
SAMSs' groups maximum number m out of n SAMSs' total number Maximum number m of SAMS groups from a total of n SAMSs	ξ_m
Intensity of transition from state S_i to state Sj of a Markov process	ξ_{ij}

The number (j) of SAMS that can fire at MAA in a particular area determines the layering of fire zone in that area. The number ξ_j of sectors with j-th layering in the fire zone of the SAMS group does not exceed the number of combinations C_n^j.

$$\xi_j = C_n^j = \frac{n!}{j!(n-j)!} \qquad 0 \le j \le n \tag{1}$$

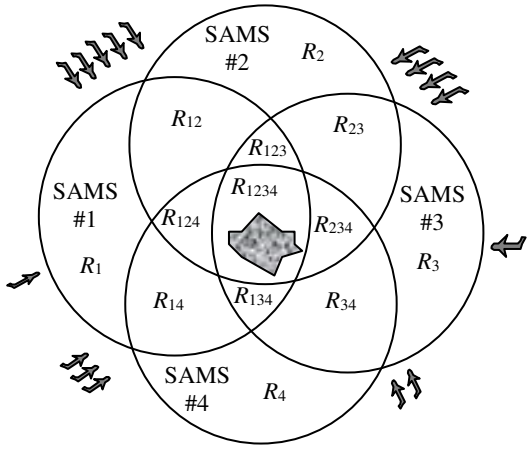

Fig. 1 An example of projecting the fire zone of a SAMS grouping onto Earth's surface

If, at a given section of the group's fire zone, all SAMS are already engaged with targets when a new MAA appears, the new MAA will pass through the fire zone unchallenged – effectively denied engagement. At the same time, other SAMS in grouping may be free at this point in time, but for them the new MAA will not be accessible for firing.

The approximately identical sizes and configuration of areas with *j*-th layering in the fire zone (Fig. 1) of the SAMS grouping allow us to consider the hypothesis about the approximate equality of probabilities of MAA hitting in such sectors as non-contradictory.

$$R_{i_1 \ldots i_j} = l_j \tag{2}$$

The probability of MAA hitting at least one of the areas with *j*-th layering can be estimated as the ratio of total area of such sectors to the total area of SAMS group fire zone.

$$\pi_j = \frac{z_j}{z_\Sigma} \qquad 0 \le j \le n \tag{3}$$

On the other hand, such a probability will be equal to the sum of probabilities of getting to each of sections with the *j*-th layering:

$$\pi_j = \sum_{i=1}^{\xi_j} l_j = \xi_j l_j = C_n^j l_j \qquad 0 \le j \le n \tag{4}$$

Eqs (1)-(4) enable to find an estimate of MAA hitting probability into a section of fire zone with the *j*-th layering.

$$l_j = \frac{z_j}{C_n^j z_\Sigma} = \frac{\pi_j}{C_n^j} \qquad 0 \le j \le n \tag{5}$$

In turn, MAAs carry out their tasks in combat formations as part of tactical groups of various purposes [1] according to r ($r = 1, 2, ..., L$) MAA in a group. In each group, the number of MAAs can be determined by the value of polygon outfit to overcome the fire zone of the SAMS group and to destroy the corresponding object. The

number n_r of possible typical objects to be hit by an air blow and the total number N_{obj} of objects to be hit during an MAA strike allow us to estimate the probability of having MAA groups with exactly r MAA in a group during an air blow.

$$b_r = \frac{n_r}{N_{obj}} \qquad 1 \le r \le L \tag{6}$$

The moments of each MAA group appearance in the fire zone of the SAMS grouping are not known in advance – they are random. The totality of such moments generates a total flow of MAA groups, random for the SAMS grouping, with a composition in each MAA group that is not known in advance for the SAMS grouping, with flow intensity I, with density $f_1(t) = Ie^{-It}$ and with flow parameter λ, which includes partial flows of MAA groups with parameters λ_r

$$\lambda_r = \lambda b_r \quad r = \overline{1,L} \quad M_{in.gr} = \sum_{r=1}^{L} r b_r \quad \lambda_r = \sum_{r=1}^{L} \lambda_r \quad I = \sum_{r=1}^{L} r\lambda_r \tag{7}$$

The limited accessibility of SAMS group properties for engaging MAA, as established in [1] and observed in practice, along with the unknown number of MAA in each subsequent group, results in impact loads and diminishes the effectiveness of SAMS groupings in carrying out their combat missions. As a result, there is a need to build a model while simultaneously taking into account the noted properties during the execution of tasks by the SAMS grouping, which makes the research topic relevant.

The shelling of each MAA by each SAMS of the SAMS group takes an unknown time with an average value $T = \mu^{-1}$ and with a distribution density $f_2(t) = \mu e^{-\mu t}$.

The exponential distribution of SAMS firing cycle duration and the time intervals between MAA groups upon entering the SAMS grouping fire zone determine the possibility of applying elements of Markov processes with continuous time and discrete states theory to construct the desired model

When assessing the potential capabilities of the SAMS grouping to repel an MAA strike, the possibility of destroying SAMS in grouping is not considered and can be considered further using the ideas outlined in [1].

2 Preliminaries and Related Works

The literature presents works aimed at modeling the execution of tasks by air defense and missile defense systems in the protection of ground targets [2-5] and naval groups [6] using elements of queuing theory with the simplest flows of demands [2, 6], using the idea of heterogeneous networks [4], Petri nets [5] and game theory [3]. In the noted and similar works on assessing the capabilities of SAMS (and missile defense) groups, the properties of incomplete accessibility of the grouping and the group composition of MAA in strikes were not considered. Each of the noted properties is considered separately in detail when constructing models in [7] and [8]. However, a joint consideration of a real process' both properties when assessing the potential capabilities of SAMS groups is not presented in the literature.

Therefore, the purpose of this research is to obtain an analytical description of the model for assessing the potential capabilities of anti-aircraft missile forces grouping to repel air strikes while simultaneously considering the group composition of MAA in the strike and the incomplete accessibility of SAMS group for shelling MAA.

3 Research Results

3.1 Theorem and Rule for Writing Equations for Groups of Markov Graph States

Due to the high complexity of formalizing real processes with the aforementioned properties, it is necessary to first examine some general characteristics of Markov processes through graphical representations – such as a Markov graph (Fig. 2). Let us define the concept of "transition flow" along a graph edge $S_i - S_j$ (Fig. 2) as the product of transitions intensity ξ_{ij} along this edge (along the arrow) by the probability P_i of the state from which the graph arrow exits

$$P_i \cdot \xi_{ij} \tag{8}$$

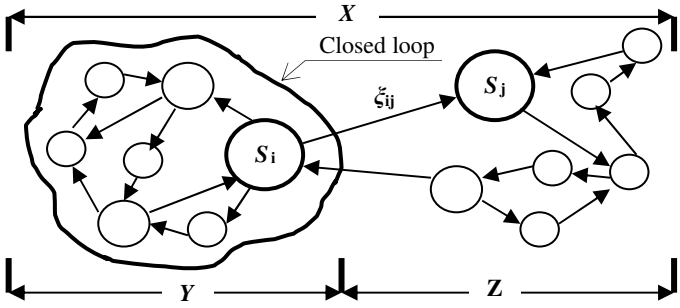

Fig. 2 Graph of Markov process model

In this wording, we can formulate the following theorem. The derivative of finding process probability in a subset of graph vertices, covered by a closed contour, does not depend on the transition flows within the subset of vertices and is equal to the algebraic sum of the transition flows along the edges of the graph intersecting the partition contour. Incoming flows will have a plus sign; outgoing flows will have a minus sign.

To prove the theorem, we divide the set of graph vertices X by a closed contour into two disjoint subsets Y and Z (Fig. 2).

$$Y \cap Z = 0 \qquad Y = X - Z \tag{9}$$

Let us denote the probabilities (P_X, P_Y, P_Z) of finding the Markov process in each subset of vertices:

$$P_Y(t) = \sum_{i \in Y} P_i(t) \qquad P_Z(t) = \sum_{i \in Z} P_i(t) \qquad P_X(t) = P_Y(t) + P_Z(t) = \sum_{i \in X} P_i(t) = 1 \tag{10}$$

and differentiate Eqs. (10):

$$\dot{P}_Y(t) = \sum_{i \in Y} \dot{P}_i(t) \qquad \dot{P}_Z(t) = \sum_{i \in Z} \dot{P}_i(t) \qquad \dot{P}_X(t) = \dot{P}_Y(t) + \dot{P}_Z(t) = \sum_{i \in X} \dot{P}_i(t) = 0 \tag{11}$$

For the probability of a Markov process being at any i-th vertex, the Kolmogorov differential equation is valid

$$\dot{P}_i(t) = -P_i(t) \sum_{k \in X} \xi_{ik} + \sum_{k \in X} P_k(t) \xi_{ki} \tag{12}$$

Let us substitute Eq. (12) into Eq. (11) and get

$$\dot{P}_Y(t) = \sum_{i\in Y}\left[-P_i(t)\sum_{k\in Y}\xi_{ik} + \sum_{k\in Y}P_k(t)\xi_{ki}\right] - \sum_{i\in Y}\left(P_i(t)\sum_{j\in Z}\xi_{ij}\right) + \sum_{j\in Z}\left(P_j(t)\sum_{k\in Y}\xi_{jk}\right) \quad (13)$$

$$\dot{P}_Z(t) = \sum_{i\in Z}\left[-P_i(t)\sum_{k\in Z}\xi_{ik} + \sum_{k\in Z}P_k(t)\xi_{ki}\right] - \sum_{j\in Z}\left(P_j(t)\sum_{k\in Y}\xi_{jk}\right) + \sum_{i\in Y}\left(P_i(t)\sum_{j\in Z}\xi_{ij}\right) \quad (14)$$

$$\dot{P}_X(t) = \sum_{i\in Y}\left[-P_i(t)\sum_{k\in Y}\xi_{ik} + \sum_{k\in Y}P_k(t)\xi_{ki}\right] + \sum_{i\in Z}\left[-P_i(t)\sum_{k\in Z}\xi_{ik} + \sum_{k\in Z}P_k(t)\xi_{ki}\right] = 0 \quad (15)$$

Eq. (15) considers the fact that when summing in Eqs (13) and (14), the expressions outside the brackets cancel each other out.

From Eq. (15) it follows:

$$-\sum_{i\in Y}\left[-P_i(t)\sum_{k\in Y}\xi_{ik} + \sum_{k\in Y}P_k(t)\xi_{ki}\right] = \sum_{i\in Z}\left[-P_i(t)\sum_{k\in Z}\xi_{ik} + \sum_{k\in Z}P_k(t)\xi_{ki}\right] \quad (16)$$

Since in the left part of Eq. (16) there is no intensity ξ_{ij} for which the index i or j belongs to the set of vertices Z, and in the right part there is no intensity ξ_{ij} for which the index i or j belongs to the set of vertices Y, then Eq. (16) is possible only under the condition that the left and right parts of Eq. (16) are equal to zero.

$$-\sum_{i\in Y}\left[-P_i(t)\sum_{k\in Y}\xi_{ik} + \sum_{k\in Y}P_k(t)\xi_{ki}\right] = 0 \quad \sum_{i\in Z}\left[-P_i(t)\sum_{k\in Z}\xi_{ik} + \sum_{k\in Z}P_k(t)\xi_{ki}\right] = 0 \quad (17)$$

Eq. (17) allow us to assert that in the right-hand sides of formulas (13) and (14) of differential equations for Markov graph groups of states, only terms for transition flows along the edges of graph intersecting the partition contour remain, and the outgoing flows have a minus sign, and the incoming flows have a plus sign:

$$\left.\begin{aligned}\dot{P}_Y(t) &= -\sum_{i\in Y}P_i(t)\sum_{j\in Z}\xi_{ik} + \sum_{j\in Z}P_j(t)\sum_{k\in Y}\xi_{ik}\\ \dot{P}_Z(t) &= -\sum_{j\in Z}P_j(t)\sum_{k\in Y}\xi_{ik} + \sum_{i\in Y}P_i(t)\sum_{j\in Z}\xi_{ik}\end{aligned}\right\} \quad (18)$$

The theorem is proved. From Eq. (18) follows the statement that in the stationary mode, the probabilities derivatives of the process being in the state groups are equal to zero.

$$\dot{P}_Y(t) = \dot{P}_Z(t) = 0 \quad (19)$$

From Eq. (18) it also follows that in a steady state, the total flow of transitions through any closed loop on a Markov graph is equal to zero.

$$-\sum_{i\in Y}P_i\sum_{j\in Z}\xi_{ij} + \sum_{j\in Z}P_j\sum_{k\in Y}\xi_{jk} = 0 \quad (20)$$

Eq. (20) allows us to formulate a rule for compiling equations for the balance of transition flows.

For a steady-state (stationary) regime, the sum of the transition flows entering the closed loop on the Markov graph of process states is equal to the sum of the outgoing transition flows.

$$\sum_{j\in Z} P_j \sum_{k\in Y} \xi_{jk} = \sum_{i\in Y} P_i \sum_{j\in Z} \xi_{ij} \tag{21}$$

3.2 Model for Assessing Potential Capabilities of a SAM Systems Group

Under the considered conditions (1)-(7), the process of executing tasks by the SAMS group can be represented by Markov model of an *n*-channel queuing system (QS) of MAA groups flow with refusals and with not fully accessible channels.

Each MAA group, while passing through the fire zone of a SAMS grouping, may find itself in the fire zone of any of the SAMS groups with specific numbers $j_1, ..., j_k$. One SAMS is assigned to fire at each MAA in the group. If insufficient SAMS are available in the zone, part of the MAA may pass through the SAMS group's engagement zone without interception (i.e., service is denied). Possible states $S_{i_1 \ldots i_k}$ of the SAMS grouping are determined by number k and specific numbers $i_1, .., i_k$ of occupied SAMS.

A fragment of such a model's graph for conditions $n = 4$ is presented in Fig. 3. A tier of the model graph is a group state of the system, which includes a set C_n^k of its possible states with the same number k of occupied SAMS.

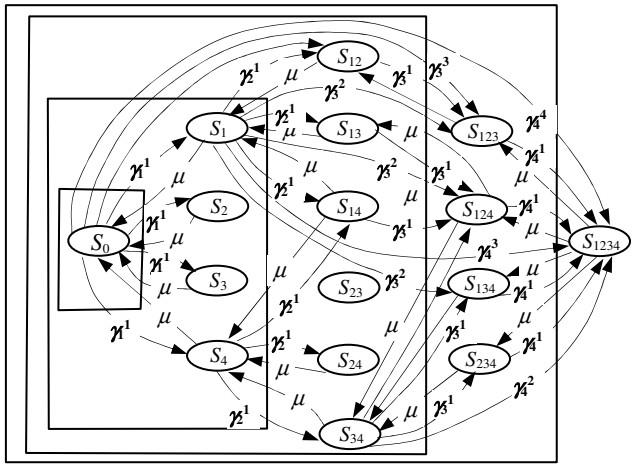

Fig. 3 Fragment of requirements groups flow service model graph by non-fully accessible QS with refusals

To indicate the intensities of transitions between tiers, the lower index indicates the absolute number of the tier to which the transition arc leads, and the upper index indicates the number of tiers through which the transition arc "jumps", taking into account the final tier. Thus, the designation γ_4^3 shows (Fig. 3) the intensity of the transition to the state S_{1234} of the fourth tier from the state S_1 of the first tier.

Let us consider the logic of determining the intensities of transitions between the states of the graph tiers (Fig. 3).

Thus, the transition from one state S_0 to another S_1 becomes possible when single MAAs (partial flow parameter λ_1) enter the system and provided that these MAAs enter the zone of SAMS groups (service channels) in which channel number "1" participates. In this case, the probability of choosing any channel, including channel

number 1, is inversely proportional to the number of free channels in this fire zone (in the service area). The subscript denotes the initial and final states between which the transition intensity is estimated.

$$\gamma^1_{0\to 1} = \lambda_1\left[R_1 + \frac{1}{2}\left(R_{12}+R_{13}+R_{14}\right) + \frac{1}{3}\left(R_{123}+R_{124}+R_{134}\right) + \frac{1}{4}R_{1234}\right] + R_1\sum_{r=2}^{L}\lambda_r \quad (22)$$

$$\gamma^1_{1\to 12} = \lambda_1\left[R_2 + R_{12} + \frac{1}{2}\left(R_{23}+R_{24}\right) + \frac{1}{2}\left(R_{123}+R_{124}\right) + \frac{1}{3}R_{234} + \frac{1}{3}R_{1234}\right] + \left(R_2+R_{12}\right)\sum_{r=2}^{L}\lambda_r \quad (23)$$

$$\gamma^1_{12\to 123} = \lambda_1\left[R_3 + R_{23} + R_{13} + \frac{1}{2}R_{34} + R_{123} + \frac{1}{2}\left(R_{134}+R_{234}\right) + \frac{1}{2}R_{1234}\right] + \left(R_3+R_{13}+R_{23}+R_{123}\right)\sum_{r=2}^{L}\lambda_r \quad (24)$$

$$\gamma^1_{123\to 1234} = \lambda_1\left[R_4 + R_{14} + R_{24} + R_{34} + R_{124} + R_{134} + R_{234} + R_{1234}\right] + \left(R_4+R_{14}+R_{24}+R_{34}+R_{124}+R_{134}+R_{234}+R_{1234}\right)\sum_{r=2}^{L}\lambda_r \quad (25)$$

Next, we consider the hypothesis (2) about the approximate equality of MAA getting probabilities into areas with the same layering and obtain

$$\gamma^1_{0\to 1} = \gamma^1_{0\to 2} = \ldots = \gamma^1_1 = \lambda_1\left(l_1 + \frac{3}{2}l_2 + l_3 + \frac{1}{4}l_4\right) + l_1\sum_{r=2}^{L}\lambda_r \quad (26)$$

$$\gamma^1_{1\to 12} = \gamma^1_{1\to 13} = \ldots = \gamma^1_2 = \lambda_1\left(l_1 + 2l_2 + \frac{4}{3}l_3 + \frac{1}{3}l_4\right) + \left(l_1+l_2\right)\sum_{r=2}^{L}\lambda_r \quad (27)$$

$$\gamma^1_{12\to 123} = \gamma^1_{12\to 124} = \ldots = \gamma^1_3 = \lambda_1\left(l_1 + \frac{2}{5}l_2 + 2l_3 + \frac{1}{2}l_4\right) + \left(l_1+2l_2+l_3\right)\sum_{r=2}^{L}\lambda_r \quad (28)$$

$$\gamma^1_{123\to 1234} = \gamma^1_{124\to 1234} = \ldots = \gamma^1_4 = \lambda_1\left(l_1+3l_2+3l_3+l_4\right) + \left(l_1+3l_2+3l_3+l_4\right)\sum_{r=2}^{L}\lambda_r \quad (29)$$

For the general case we find:

$$\gamma^1_k = \lambda_1\sum_{j=1}^{n}\left[l_j\sum_{i=0}^{j-1}\frac{1}{C^1_{i+1}}C^{j-1-i}_{k-1}C^i_{n-k}\right] + \left(\sum_{j=0}^{k-1}l_{j+1}C^j_{k-1}\right)\sum_{r=2}^{L}\lambda_r \quad (30)$$

For the case of transition through one state, we find the intensity similarly:

$$\gamma^2_{0\to 12} = \lambda_2\left(R_{12} + \frac{1}{3}\cdot R_{123} + \frac{1}{3}R_{124} + \frac{1}{6}R_{1234}\right) + R_{12}\sum_{r=3}^{L}\lambda_r \quad (31)$$

$$\gamma^2_{1\to 123} = \lambda_2\left(R_{23} + R_{123} + \frac{1}{3}R_{234} + \frac{1}{3}R_{1234}\right) + \left(R_{12}+R_{123}\right)\sum_{r=3}^{L}\lambda_r \quad (32)$$

$$\gamma^2_{12\to1234} = \lambda_2\left(R_{34} + R_{134} + R_{234} + R_{1234}\right) + \left(R_{34} + R_{134} + R_{234} + R_{1234}\right)\sum_{r=3}^{L}\lambda_r \quad (33)$$

After taking into account Eq. (2), Eqs (31)-(33) will take the following form:

$$\gamma^2_{0\to12} = \gamma^2_{0\to13} = ... = \gamma^2_2 = \lambda_2\left(l_2 + \frac{2}{3}l_3 + \frac{1}{6}l_4\right) + l_2\sum_{r=3}^{L}\lambda_r \quad (34)$$

$$\gamma^2_{1\to123} = \gamma^2_{1\to124} = ... = \gamma^2_3 = \lambda_2\left(l_2 + \frac{4}{3}l_3 + \frac{1}{3}l_4\right) + \left(l_2 + l_3\right)\sum_{r=3}^{L}\lambda_r \quad (35)$$

$$\gamma^2_{12\to1234} = \gamma^2_{13\to1234} = ... = \gamma^2_4 = \lambda_2\left(l_2 + 2l_3 + l_4\right) + \left(l_2 + 2l_3 + l_4\right)\sum_{r=3}^{L}\lambda_r \quad (36)$$

In steps, expressions (34)-(36) can be represented as follows:

$$\gamma^2_k = \lambda_2\sum_{j=1}^{n}\left[l_j\sum_{i=0}^{j-2}\frac{1}{C^2_{i+2}}C^{j-2-i}_{k-2}C^i_{n-k}\right] + \left[\sum_{j=0}^{k-2}l_{j+2}C^j_{k-2}\right]\sum_{r=3}^{L}\lambda_r \quad (37)$$

By comparing expressions (30) and (37), one can obtain a calculation expression for the intensity of transitions between graph tiers (Fig. 3) in general case:

$$\gamma^q_k = \lambda_q\sum_{j=1}^{n}\left[l_j\sum_{i=0}^{j-q}\frac{1}{C^q_{i+q}}C^{j-q-i}_{k-q}C^i_{n-k}\right] + \left[\sum_{j=0}^{k-q}l_{j+q}C^j_{k-q}\right]\sum_{r=q+1}^{L}\lambda_r, \quad \begin{cases} q = \overline{1,\cdots,n} \\ k = \overline{1,\cdots,n} \end{cases} \quad (38)$$

To form group states of repelling strikes process by the SAMS group and the corresponding probabilities, we will combine states with the same number of occupied channels using the example of the model graph in Fig. 3

$$\left.\begin{aligned} P_0 &= p_0 \\ P_1 &= p_1 + p_2 + p_3 + p_4 \\ P_2 &= p_{12} + p_{13} + p_{14} + p_{23} + p_{24} + p_{34} \\ P_3 &= p_{123} + p_{124} + p_{134} + p_{234} \\ P_4 &= p_{1234} \end{aligned}\right\} \quad (39)$$

In order to find the final probabilities of group states, we will use the consequence of theorem (18) and step by step compose the equations of the balance of transition flows (21) for a sequence of nested closed contours (Fig. 3). For the inner contour we get:

$$\mu p_1 + \mu p_2 + \mu p_3 + \mu p_4 = \left(4\gamma^1_1 + 6\gamma^2_2 + 4\gamma^3_3 + 1\gamma^4_4\right)p_0 \quad (40)$$

Considering the fixed number $n = 4$ of channels in grouping, as well as Eqs (1) and (39), expression (40) takes the form:

$$\mu P_1 = P_0\left(C^1_n\gamma^1_1 + C^2_n\gamma^2_2 + C^3_n\gamma^3_3 + C^4_n\gamma^4_4\right) \quad (41)$$

Using similar reasoning, we will formulate the balance equations for the transition flows along the remaining closed contours in the model graph (Fig. 3), obtaining

$$\left.\begin{aligned} 2\mu P_2 &= P_1\left(3\gamma^1_2 + 3\gamma^2_3 + 1\gamma^3_4\right) + P_0\left(6\gamma^2_2 + 4\gamma^3_3 + 1\gamma^4_4\right) \\ 2\mu P_2 &= P_1\left(C^1_{n\text{-}1}\gamma^1_2 + C^2_{n\text{-}1}\gamma^2_3 + C^3_{n\text{-}1}\gamma^3_4\right) + P_0\left(C^2_n\gamma^2_2 + C^3_n\gamma^3_3 + C^4_n\gamma^4_4\right) \end{aligned}\right\} \quad (42)$$

$$\begin{aligned} 3\mu P_3 &= P_2\left(2\gamma_3^1 + 1\gamma_4^2\right) + P_1\left(3\gamma_3^2 + 1\gamma_4^3\right) + P_0\left(4\gamma_3^3 + 1\gamma_4^4\right) \\ 3\mu P_3 &= P_2\left(C_{n-2}^1\gamma_3^1 + C_{n-2}^2\gamma_4^2\right) + P_1\left(C_{n-1}^2\gamma_3^2 + C_{n-1}^3\gamma_4^3\right) + P_0\left(C_n^3\gamma_3^3 + C_n^4\gamma_4^4\right) \end{aligned} \quad (43)$$

$$\begin{aligned} 4\mu P_4 &= P_3 1\gamma_4^1 + P_2 1\gamma_4^2 + P_1 1\gamma_4^3 + P_0 1\gamma_4^4 \\ 4\mu P_4 &= P_3 C_{n-3}^1\gamma_4^1 + P_2 C_{n-2}^1\gamma_4^2 + P_1 C_{n-1}^1\gamma_4^3 + P_0 C_n^1\gamma_4^4 \end{aligned} \quad (44)$$

The regularities that can be observed in Eqs (42)-(44) allow us to write the equation for the balance of transition flows for the general case as follows:

$$k\mu P_k = \sum_{j=1}^{k}\left(P_{k-j}\sum_{q=j}^{n-k+j} C_{n-k+j}^q \cdot \gamma_{k-j+q}^q\right) \quad (45)$$

We will search for the calculation expressions for the final probabilities of group states in a form close to the Erlang formulas and using the deformation function F_k of the final probabilities:

$$\left.\begin{aligned} P_k &= P_0\frac{(\rho_1)^k}{k!}F_k, \qquad k = \overline{1,\cdots,n} \\ P_0 &= \left(\sum_{k=0}^{n}\frac{(\rho_1)^k}{k!}F_k\right)^{-1} \\ \rho_q &= \frac{\lambda_q}{\mu}, \qquad q = \overline{1,\cdots,n} \end{aligned}\right\} \quad (46)$$

In order to reduce the length of the equations, we introduce a notation for the intensity of transitions d_k^q in Eq. (38).

$$d_k^q = \left\{\sum_{j=1}^{n}\left[l_j\sum_{i=0}^{j-q}\frac{1}{C_{i+q}^q}C_{k-q}^{j-q-i}C_{n-k}^i\right] + \frac{1}{\lambda_q}\left[\sum_{j=0}^{k-q}l_{j+q}C_{k-q}^j\right]\sum_{r=q+1}^{L}\lambda_r\right\}, \quad \begin{cases} q = \overline{1,\cdots,n} \\ k = \overline{1,\cdots,n} \end{cases} \quad (47)$$

Then Eq. (38) will take the form:

$$\gamma_k^q = \lambda_q d_k^q, \qquad \begin{cases} q = \overline{1,\cdots,n} \\ k = \overline{1,\cdots,n} \end{cases} \quad (48)$$

Let us substitute the expression for the final probabilities P_k (46) into Eq. (45).

$$k\mu P_0\frac{(\rho_1)^k}{k!}F_k = \sum_{j=1}^{k}P_0\frac{(\rho_1)^{k-j}}{(k-j)!}F_{k-j}\sum_{q=j}^{n-k+j}C_{n-k+j}^q\lambda_q d_{k-j+q}^q \quad (49)$$

Eq. (49) allows us to find the calculation expression for the deformation functions.

$$F_k = \sum_{j=1}^{k}F_{k-j}\frac{(k-1)!}{(\rho_1)^j(k-j)!}\sum_{q=j}^{n-k+j}C_{n-k+j}^q\rho_q d_{k-j+q}^q, \qquad k = \overline{1,\cdots,n} \quad (50)$$

In order to find the initial value F_0 of deformation function, we use expression (45) with the value $k = 1$.

$$\mu P_1 = P_0 \sum_{q=1}^{n} C_n^q \lambda_q d_q^q \tag{51}$$

Considering Eq. (46), Eq. (51) takes the following form:

$$\mu P_0 \rho_1 F_1 = P_0 \sum_{q=1}^{n} C_n^q \lambda_q d_q^q \tag{52}$$

From Eq. (51), considering the Eq. in (46), we find

$$F_1 = \frac{1}{\rho_1} \sum_{q=1}^{n} C_n^q \rho_q d_q^q \tag{53}$$

From Eq. (50) with the value $k = 1$ we find

$$F_1 = F_0 \frac{1}{\rho_1} \sum_{q=1}^{n} C_n^q \rho_q d_q^q \tag{54}$$

After comparing the right-hand sides of Eqs (53) and (54), we obtain:

$$\frac{1}{\rho_1} \sum_{q=1}^{n} C_n^q \rho_q d_q^q = F_0 \frac{1}{\rho_1} \sum_{q=1}^{n} C_n^q \rho_q d_q^q \tag{55}$$

Eq. (55) allows us to find the value of the initial function:

$$F_0 = 1 \tag{56}$$

Expressions (56), (50), (47), and (38) are an analytical description of the desired model for assessing the potential capabilities of SAMS grouping to repel air strikes while simultaneously taking into account the group composition of MAA in the strike and the incomplete accessibility of the SAMS group for firing at MAA, which allows us to consider the goal of the research as achieved.

3.3 Verification of Model for Assessing SAMS Group Potential Capabilities

At the first stage of obtained model verification, we will check the correctness of its main calculation expressions (50) and (46) by modifying it (simplifying it) to the level of known particular models that have already passed the check of their correctness.

Thus, if the positions of all SAMS of the SAMS grouping are located at one point, any MAA will be accessible for shelling by any free SAMS, therefore, from formulas (5) we find:

$$\left.\begin{aligned} l_k &= \frac{\pi_k}{C_n^k} = 0, \quad k < n \\ l_n &= \frac{\pi_n}{C_n^n} = \pi_n = 1 \end{aligned}\right\} \tag{57}$$

Next, step by step, Eq. (45) is transformed into Eq. (58)

$$k\mu P_k = \sum_{j=1}^{k} P_{k-j} \left[\sum_{q=j}^{n-k+j-1} \left(\lambda_q \frac{C_{n-k+j}^q}{C_{n-k+j}^q} + 0 \right) + C_{n-k+j}^{n-k+j} \cdot 0 \cdot \sum_{r=q+1}^{L} \lambda_r \right] \tag{58}$$

and finally takes the form

$$k\mu P_k = \sum_{j=1}^{k} P_{k-j} \sum_{q=j}^{L} \lambda_q \tag{59}$$

Expression (59) represents the same fundamental equality as Eq. (45), but applied to the validated model [7], which assumes full accessibility of service channels and an input flow consisting of groups of requirements. In this case, the deformation functions in expressions (50) are automatically transformed into the non-ordinarity functions, as defined in [7, Eq. (18)].

In the case of the appearance of only single MAAs in the strike and the placement of SAMS in combat formation on the terrain while maintaining incomplete accessibility of the SAMS grouping for firing at MAAs, in equalities (6), the probability of single MAAs appearance will be equal to one ($b_1 = 1$).

All other probabilities become equal to zero ($b_r = 0$, $r = 2,\ldots, L$). Then the parameter of the first partial MAA flow will be equal to the intensity of the input MAA flow ($\lambda_1 = I$), and the parameters of the remaining flows become equal to zero ($\lambda_r = 0$, $r \geq 2$).

Therefore, in Eq. (38) for the condition all $q \geq 2$ values except the first value will be equal to zero $\gamma_k^q = 0$. In the basic equality (45) the internal sum will be non-zero only for the condition $j = 1$, which will lead to a new form of equality (45)

$$k\mu P_k = P_{k-1} C_{n-k+1}^1 \tag{60}$$

Eq. (60) represents the same basic equality as Eq. (45), but for the verified model [8] with partial accessibility of service channels and with the simplest input flow of requirements. In this case, the expression for the deformation functions (50) is automatically transformed into the expression for the function representing the partial accessibility of service channels [8, Eq. (28)].

Thus, the analytical description of the considered combat model is a general case for particular verified models, which consider only one of the noted properties of repelling MAA strikes process by the SAMS grouping.

At the second stage of obtained model analytical description verification, we will calculate the expected effectiveness of covering an object with a grouping of four single-channel SAMS (Fig. 1). This SAMS grouping is engaged in air-defense battle during 10 minutes with enemy's groups of manned and unmanned MAAs consisting of 22 MAAs. The intensity of enemy air blow is 2.2 MAAs/minute (Tab. 1 items 2-8, 15-20).

Overcoming the grouping's fire zone with more than eight MAAs allows the enemy to defeat the protected object. If less than eight MAAs of the enemy break through to the object, the SAMS grouping's mission is considered accomplished.

In case of simultaneous employment of all SAMS in SAMS grouping at the moment of entry the next MAA into fire zone, such MAA may be denied fire and pass through the grouping's fire zone without damage. The mathematical expectation of such MAAs number (N_{missed}) can be found using the probability of opposite event - probability of servicing MAA by SAMS grouping

$$N_{\text{missed}} = N_{\text{total.En}} \left(1 - P_{\text{service}}\right) \tag{61}$$

In turn, the service probability (P_{service}) can be found after calculating the probabilities (P_k) of the group states of the SAMS grouping (46) during the battle and after estimating the mathematical expectation of the number of SAMS occupied during the battle

$$M_{b.\mathrm{SAM}} = \sum_{k=0}^{n} kP_{\mathrm{k}} \qquad P_{\mathrm{service}} = \frac{\mu M_{b.\mathrm{SAM}}}{I} \tag{62}$$

The initial data for the calculations are presented in Tab. 1 items 1-13. The intensities of transitions between the tiers of the model graph (Fig. 3) are found using Eq. (38).

$$\gamma_1^1 = \lambda_1\left(l_1 + \frac{3}{2}l_2 + l_3 + \frac{1}{4}l_4\right) + l_1\sum_{i=2}^{5}\lambda_i \tag{63}$$

$$\gamma_2^1 = \lambda_1\left(l_1 + 2l_2 + \frac{4}{3}l_3 + \frac{1}{3}l_4\right) + (l_1 + l_2)\sum_{i=2}^{5}\lambda_i \tag{64}$$

$$\gamma_2^2 = \lambda_2\left(l_2 + \frac{2}{3}l_3 + \frac{1}{6}l_4\right) + l_2\sum_{i=3}^{5}\lambda_i \tag{65}$$

$$\gamma_3^1 = \lambda_1\left(l_1 + \frac{2}{5}l_2 + 2l_3 + \frac{1}{2}l_4\right) + (l_1 + 2l_2 + l_3)\sum_{i=2}^{5}\lambda_i \tag{66}$$

$$\gamma_3^2 = \lambda_2\left(l_2 + \frac{4}{3}l_3 + \frac{1}{3}l_4\right) + (l_2 + l_3)\sum_{i=3}^{5}\lambda_{\mathrm{i}} \tag{67}$$

$$\gamma_3^3 = \lambda_3\left(l_3 + \frac{1}{4}l_4\right) + l_3\sum_{r=4}^{L}\lambda_r \tag{68}$$

$$\gamma_4^1 = \lambda_1(l_1 + 3\cdot l_2 + 3l_3 + l_4) + (l_1 + 3l_2 + 3l_3 + l_4)\sum_{i=2}^{5}\lambda_i \tag{69}$$

$$\gamma_4^2 = \lambda_2(l_2 + 2\cdot l_3 + l_4) + (l_2 + 2l_3 + l_4)\sum_{i=3}^{5}\lambda_i \tag{70}$$

$$\gamma_4^3 = \lambda_3(l_3 + l_4) + l_4\sum_{i=4}^{L}\lambda_r \tag{71}$$

$$\gamma_4^4 = \lambda_4 l_4 + l_4\sum_{i=5}^{L}\lambda_r \tag{72}$$

Using the recurrence relation in Eq. (50), we derive the expressions needed to calculate the missing deformation functions in the final probabilities given by Eq. (46). Calculation of final probabilities (P_k) values (46) is possible if data on all deformation functions (F_k) are available. We will find formulas for the missing deformation functions using the recurrent expression (50)

$$F_2 = F_1\cdot\frac{1}{\lambda_1}\left(3\gamma_2^1 + 3\gamma_3^2 + 1\gamma_4^3\right) + F_0\frac{\mu}{(\lambda_1)^2}\left(6\gamma_2^2 + 4\gamma_3^3 + 1\gamma_4^4\right) \tag{73}$$

$$F_3 = F_2 \frac{1}{\lambda_1}\left(2\gamma_3^1 + 1\gamma_4^2\right) + F_1 \frac{2\mu}{(\lambda_1)^2}\left(3\gamma_3^2 + 1\gamma_4^3\right) + F_0 \frac{2\mu^2}{(\lambda_1)^3}\left(4\gamma_3^3 + 1\gamma_4^4\right) \tag{74}$$

$$F_4 = F_3 \frac{1}{(\lambda_1)^1}\gamma_4^1 + F_2 \frac{3\mu^1}{(\lambda_1)^2}\gamma_4^2 + F_1 \frac{6\mu^2}{(\lambda_1)^3}\gamma_4^3 + F_0 \frac{6\mu^3}{(\lambda_1)^4}\gamma_4^4 \tag{75}$$

In a number of cases, to assess the efficiency of task performance by the SAMS grouping, researchers use the well-known formulas of Erlang model [9], which are also applicable for performing a comparative assessment of existing and developed models

$$\left.\begin{aligned} P_k &= P_0 \frac{\rho^k}{k!}, \qquad k = \overline{1,\cdots,n} \\ P_0 &= \left(\sum_{k=0}^{n} \frac{\rho^k}{k!}\right)^{-1} \end{aligned}\right\} \tag{76}$$

The results of calculations of model parameters (Tab. 1, items 14-34) and predicted values of intermediate (Tab. 1, items 35-46) and final performance indicators (Tab. 1, items 47, 48) based on the input data (Tab. 1, items 1-13) are presented in Tab. 1 and in Figs 4 and 5. In Tab. 1 and in Figs 4 and 5, the short designation of the developed model (Dvl.) and known models (Inac., Gr., Erl.) is used, which take into account only separate properties of the anti-aircraft combat process of the SAMS grouping. The use of known models leads to a significant distortion of the task performing predicted results. Thus, the expected value of the effectiveness indicator (P_{service}) of combat task by the SAMS grouping (Tab. 1 item 47) turns out to be at least one and a half times higher than the more realistic estimates obtained using the developed model, which can lead to false optimism regarding the grouping's readiness to perform tasks.

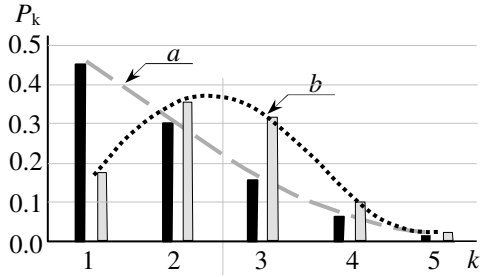

*Fig. 4 Final probabilities P_k of states' groups in models in identical conditions: a) the developed model; b) the well-known model. *Inac. – see (*) in* Tab. 1, $b_1 = 1; b_r = 0; \lambda_1 = I; \lambda_r = 0,$ for $r \geq 2$

In particular, the use of all existing models demonstrates the possibility of an object passing through with fewer than eight MAA, which meets the requirements for the successful completion of a combat mission by the SAMS grouping.

However, a more accurate consideration of combat conditions using the developed model indicates that, on average, approximately thirteen MAA are required to overcome the fire zone of the SAMS grouping (see Tab. 1, item 48).

At the same time, it can be noted that in the case of replacing four single-channel target SAMS with one SAMS with four target channels and with a sufficient size of the fire zone, the effect of full accessibility of all four channels for firing at MAA arises. In this case (Fig. 5, #3 and Tab. 1 item 47, item 48 model "Gr." see 0.638/0.397 = 1.6), the probability of completing the task increases by 1.6 times and on average less than eight MAA can break through to the object. The developed model allows such an effect to be calculated automatically when condition (57) is met: ($l_n = \pi_n = 1; l_k = 0, k < n$).

Tab. 1 Comparative assessment of task performance efficiency by SAMS grouping (Fig. 1) *using developed and known types of models*

Names and values of models' input data (1-13), forecast values of - parameters (14-34), intermediate indicators (35-46) and performance indicators (47, 48)											Types of models			
#	Name	Value	#	Name	Value	#	Name	Value	#	Name	Dvl.*	Inac.*	(Gr.)*	Erl.*
1	2	3	4	5	6	7	8	9	10	11	12	13	14	15
1	n	4	**13**	μ	1	25	γ_1^1	0.082	37	F_0	1	1	1	1
2	I	2.2	14	ρ_1	0.065	26	γ_2^1	0.114	38	F_1	10	1	10	1
3	λ	0.647	15	L	5	27	γ_3^1	0.164	39	F_2	163.25	0.888	239.09	1
4	b_1	0.100	16	λ_1	0.065	28	γ_4^1	0.306	40	F_3	3036.1	0.457	8516.5	1
5	b_2	0.200	17	λ_2	0.129	29	γ_2^2	0.035	41	F_4	49473	0.216	395982	1
6	b_3	0.200	18	λ_3	0.129	30	γ_3^2	0.058	42	P_0	0.463	0.157	0.354	0.119
7	b_4	0.200	19	λ_4	0.129	31	γ_4^2	0.128	43	P_1	0.299	0.345	0.229	0.263
8	b_5	0.300	20	λ_5	0.194	32	γ_3^3	0.021	44	P_2	0.158	0.337	0.177	0.289
9	π_1	0.45	21	l_1	0.112	33	γ_4^3	0.046	45	P_3	0.063	0.127	0.136	0.212
10	π_2	0.3	22	l_2	0.05	**34**	γ_4^4	0.029	46	P_4	0.017	0.033	0.103	0.117
11	π_3	0.16	23	l_3	0.04	35	$M_{b.SAM}$	0.872	**47**	$P_{service}$	0.397	0.697	0.638	0.883
12	π_4	0.09	24	l_4	0.09	36	$M_{in.gr.}$	3.4	**48**	N_{miss}	13.28	6.66	7.97	2.57

*Dvl. – the developed model with refusals with not fully accessible SAMS and with input flow of MAAs' groups.

*Inac. – the known model with not fully accessible service channels and with refusals. The functions F_j automatically degenerate into known incomplete accessibility functions [8, Eq. (28)].

*Gr. – the known model with input flow of requirements' groups and with refusals. The functions F_j automatically degenerate into known non-ordinary functions [7, Eq. (18)].

*Erl. – the known Erlang model with refusals. The functions F_j automatically become equal to one [9].

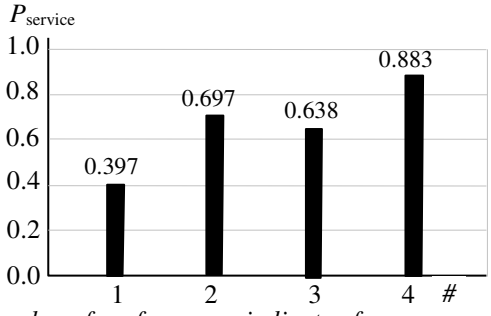

Fig. 5 Predicted value of performance indicator for a group of SAM systems (Fig. 1)*, using models: 1) the developed model; 2) the model *Inac. – see (*) in* Tab. 1*; 3) the model *Gr. – see (*) in* Tab. 1*; 4) the model *Erl – see (*) in* Tab. 1

In all cases, the deformation functions ($F_0 - F_4$) automatically degenerate into functions of incomplete accessibility (Tab. 1, items 37-41, column Inac.) and into functions of non-ordinarity (Tab. 1, items 37-41, column Gr.). Also, they take a single

value (Tab. 1, items 37-41, column Erl.) when moving to the Erlang model, with automatic calculation of final probabilities in the corresponding models. The recurrent form of the deformation functions calculation expressions (50) allows automating the process of their calculations for specific combat conditions.

4 Results

In order to build a model for assessing and forecasting the expected effectiveness of the SAMS grouping's missions, the possibility of using the Markov model of combat processes dynamics was demonstrated for the first time, while simultaneously considering the most significant features of the SAMS grouping's combat formations on the ground (not full accessibility of SAMS for MAA shelling) and MAA in the air (actions by tactical groups). An analytical description of this model became possible through the application of a proven theorem on the special properties of Markov graphs, allowing us to consider the research objective as successfully achieved.

The correctness of this model is supported by verification results, obtained by automatically transforming its analytical description into that of previously validated models, which account for only some of the considered features.

The results of the numerical experiment demonstrate the possibility of using the model to search for and justify the composition of the SAMS grouping.

5 Conclusions

An analytical description of the model for assessing the potential capabilities of anti-aircraft missile forces grouping to repel air strikes after its computer implementation allows for a quick and targeted search for a rational composition of the SAMS grouping.

The model allows selecting the parameters of the arrangement of individual SAMS in a combat formation, which affects the size of the overlap of SAMS fire zones in a grouping and also allows assessing the expected potential effectiveness of the SAMS grouping in performing tasks in the range of possible parameters of MAA combat formations in the air.

The correctness of the model is further supported by the results of a numerical experiment. The analytical description enabled more realistic estimates of the expected effectiveness of the SAMS grouping and allowed for the automatic determination of all parameter values characteristic of three specific model types: those accounting only for the partial accessibility of SAMS [8], only for the group composition of MAA [7], and the well-known Erlang model [9].

It should be noted, however, that the model presented in this study is designed to assess only the potential capabilities of the SAMS grouping, without considering the possible destruction of SAMS during combat. Incorporating this aspect of combat is possible in future research, building on the results presented in [1].

References

[1] GORODNOV, V.P. and V. OVCHARENKO. Inner Law and Models for Forecasting the Results of Air Defense Battle. *Advances in Military Technology*, 2022, **17**(2), pp. 246-261. DOI 10.3849/aimt.01564.

[2] ZHAO, Z.Q., J.X. HAO and L.J. LI. Study on Combat Effectiveness of Air Defense Missile Weapon System Based on Queuing Theory. In: *7th International Conference on Electronics and Information Engineering*. Nanjing: SPIE, 2017. DOI 10.1117/12.2266077.

[3] RAO, D.V. and M. RAVISHANKAR. A Methodology for Optimal Deployment and Effectiveness Evaluation of Air Defense Resources Using Game Theory. *Sådhanå*, 2020, **45**, pp. 1-15. DOI 10.1007/s12046-020-1293-8.

[4] DING, J., Q. ZHAO, J. LI and J. XU. Temporal Constraint Modeling and Conflict Resolving Based on the Combat Process of Air and Missile Defense System. In: *IEEE International Conference on Systems, Man and Cybernetics (SMC)*. Bari: IEEE, 2019, pp. 2684-2689. DOI 10.1109/SMC.2019.8914484.

[5] GAO, X., C. LU, J. TANG, L. FAN, Y. LING and Y. LI. An Evaluation Method of Object-Oriented Petri Net on Combat Effectiveness of Air Defense and Antimissile. In: *8th IEEE International Conference on Communication Software and Networks (ICCSN)*. Beijing: IEEE, 2016, pp. 590-596. DOI 10.1109/ICCSN.2016.7586592.

[6] ZHONG, Z. and L. ZHANG. The Combat Application of Queuing Theory Model in Formation Ship to Air Missile Air Defense Operations. *Journal of Physics: Conference Series*, 2020, **1570**, 012083. DOI 10.1088/1742-6596/1570/1/012083.

[7] GORODNOV, V. The Analytical Description of Final Probabilities for States of Queuing Systems with Input Flow of Groups of Requirements. *Radio Electronics, Computer Science, Control*, 2019, **4**(51), pp. 25-37. DOI 10.15588/1607-3274-2019-4-3.

[8] GORODNOV, V.P. and V.V. OVCHARENKO. The States' Final Probabilities Analytical Description in an Incompletely Accessible Queuing System with Refusal. *Radio Electronics, Computer Science, Control*, 2022, **2**(61), pp. 32-42. DOI 10.15588/1607-3274-2022-2-4.

[9] ERLANG, A.K. The Theory of Probabilities and Telephone Conversations. *Nyt Tidsskrift for Mathematic*, 1909, **20**, pp. 131-137.